

Three-point correlation functions in uniformly and randomly driven diffusive systems

K. Hwang, B. Schmittmann, and R. K. P. Zia

Center for Stochastic Processes in Science and Engineering and Physics Department,
Virginia Polytechnic Institute and State University, Blacksburg, Virginia 24061

(Received 5 March 1993)

Driven far away from equilibrium by both uniform and random external fields, a system of diffusing particles with short-range attractive forces displays many singular thermodynamic properties. Surprisingly, measuring pair correlations in lattice-gas models with saturation drives, we find little difference between the uniform and random cases, even though the underlying symmetries are quite distinct. Motivated by this puzzle, we study three-point correlations using both field-theoretic and simulation techniques. The continuum theory predicts the following: (a) The three-point function is nonzero only for the uniformly driven system; (b) it is odd under a parity transformation; and (c) there exists an infinite discontinuity singularity at the origin in momentum space. Simulation results are clearly consistent with these predictions. Based on these findings, we suggest several avenues for future investigations.

PACS number(s): 64.60.Cn, 64.90.+b, 66.30.Hs, 82.20.Mj

I. INTRODUCTION

Because of their broad application in biology, chemistry, and physics, nonequilibrium phenomena have attracted considerable interest in recent years. Usually, these systems involve many degrees of freedom, so that a statistical-mechanical description is unavoidable. Further, since we are typically interested in universal, or generic, behavior, we study simplified model systems which capture the essential physics of the real systems. One of the most well-known nonequilibrium models is the driven diffusive system (DDS), proposed by Katz, Lebowitz, and Spohn [1,2]. A DDS consists of a stochastic, interacting lattice gas under the influence of an external driving field. The physical system motivating this model is the fast ionic conductor [3]. In the original papers [1,2], the driving field is uniform in both space and time—a model we will refer to as a uniformly driven system (UDS). Though theoretically simple, such a system, with *periodic* boundary conditions, is basically impossible to achieve physically. Instead, driving with an ac field, or one which is random in time, is much more likely to be realizable. Since ac fields introduce a frequency scale, the resultant behavior may be much more complex than a simple stochastic process. We are thus motivated to study the *randomly* driven system (RDS).

The symmetries of an RDS are quite distinct from those of a UDS, leading to entirely different universality classes of critical behavior [4,5]. On the other hand, much of the data collected from Monte Carlo simulations of these systems driven with *infinite* fields show very little difference, *including* the critical temperature T_c . Faced with such a puzzle, we considered measuring quantities other than the traditional order parameter, two-point correlation function, and internal energy. The most obvious choice would be the steady-state current. However, we wish to explore differences in purely “static” quantities. Exploiting the very different symmetries between UDS and RDS, we recognize that all correlation func-

tions involving an odd number of particles, at *equal times*, must vanish in an RDS, especially for $T > T_c$. Focusing on the simplest one of these, we study the three-point correlation function. As a bonus, we find that, for a UDS, this quantity is generically singular at zero momenta, for all temperatures [6,7].

In Sec. II we will present detailed descriptions of these models and the measurements of some standard quantities which show that these two systems are essentially indistinguishable, even though they are driven by very different mechanisms. This puzzle provides the motivation for the search for quantities which exploit the different symmetries and *can distinguish* the two. The simplest is the three-point function. Section III is devoted to the different symmetries and Sec. IV, the theoretical background. Simulation data are presented in Sec. V, confirming many of our expectations. We end with a summary and an outlook for further investigations.

II. THE MODELS

In this section we describe the models: UDS and RDS. First, we review the basis for these models, namely, an Ising lattice gas in equilibrium [8]. Then we consider the influence of the driving fields.

For definiteness, we study systems in two dimensions, on square lattices. Each site, labeled by an index i , is either occupied by a particle, or vacant. Thus, a configuration C corresponds to a set of occupation numbers $\{n_i\}$, where $n_i = 1$ or 0 for an occupied or an empty site. Alternatively, we may use the Ising spin language $s_i = 2n_i - 1$, so that $s_i = \pm 1$. The total internal energy of a specific configuration C is given by one of the following Hamiltonians:

$$\begin{aligned} \mathcal{H}(C) &= -4J \sum_{i,j} n_i n_j, \\ \mathcal{H}(C) &= -J \sum_{i,j} s_i s_j, \end{aligned} \quad (2.1)$$

where i, j are indices of nearest-neighbor sites. For convenience, we will use the spin language in the rest of this paper. To model ions, we choose a dynamics which preserves the total particle number $N = \sum_i n_i$. To ensure that the system undergoes a second-order phase transition, we work with a half-filled lattice, i.e., fixing the overall density to be $\frac{1}{2}$. Finally, J denotes a positive exchange constant, corresponding to attractive (or ferromagnetic) interactions. Letting the system be in contact with a heat bath at temperature T , all equilibrium properties can be computed as suitable averages over the canonical distribution

$$P_{\text{eq}}(C) = Z^{-1} \exp(-\beta \mathcal{H}),$$

with $\beta = 1/k_B T$. At the Onsager critical temperature [8] $T_{c0} (\simeq 0.5673J/k_B)$, this system undergoes a spontaneous segregation transition: the disordered (high-temperature) phase separates into a high-density “liquid” and a low-density “gas” phase.

The dynamics of our model, which specifies how the system evolves from a given configuration C into a new configuration C' , is determined by transition rates or transition probabilities $\mathcal{W}[C \rightarrow C']$. These enter into the master equation for the time-dependent probability distribution $P(C, t)$:

$$\frac{\partial}{\partial t} P(C, t) = \sum_{C'} \{ \mathcal{W}[C' \rightarrow C] P(C', t) - \mathcal{W}[C \rightarrow C'] P(C, t) \}. \quad (2.2)$$

To model a system in equilibrium with a heat bath, the rates are determined by β and the internal energy difference of C and C' : $\Delta \mathcal{H} \equiv \mathcal{H}(C') - \mathcal{H}(C)$, i.e.,

$$\mathcal{W}[C \rightarrow C'] = \mathcal{W}[\beta \Delta \mathcal{H}]. \quad (2.3)$$

On the right-hand side, \mathcal{W} is an arbitrary positive function, apart from the requirement of detailed balance, i.e., $\mathcal{W}(-x) = \mathcal{W}(x)e^{-x}$. A popular choice is the Metropolis rate [9]: $\mathcal{W}(x) = \min\{1, e^{-x}\}$.

Next we consider the influence of the external fields. For UDS, the particles are driven by a field uniform in both space and time. The effect of this drive is to favor jumps along, and to suppress jumps against, the field. Choosing periodic boundary conditions (PBC), which make the lattice a torus, the system eventually reaches a nonequilibrium steady state with a nonzero current. The influence of such a field is easily incorporated by having an extra term in the rate function, i.e., $\mathcal{W} = \mathcal{W}[\beta \Delta \mathcal{H} + \epsilon E]$, where

$$\bullet \quad \epsilon = \begin{cases} -1 & \text{for jumps along } E \\ 0 & \text{for jumps transverse to } E \\ +1 & \text{for jumps against } E. \end{cases} \quad (2.4)$$

One of the first [1,2] remarkable results is that the second-order phase transition survives for all values of E , with T_c saturating at about 41% above the Onsager value [10] as $E \rightarrow \infty$. However, field-theoretic renormalization-group analyses predict that the critical behavior of this nonequilibrium steady state belongs to a

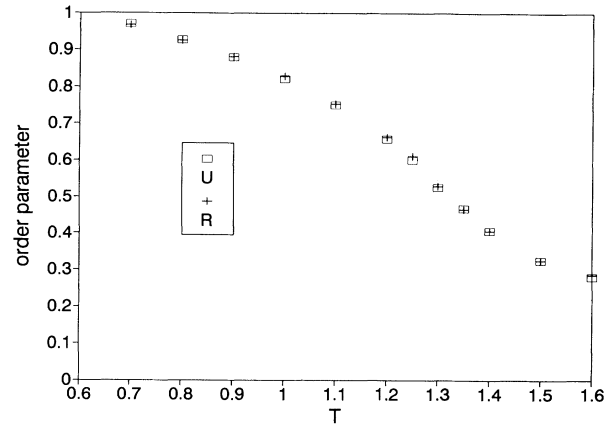


FIG. 1. Order parameters in a $L = 30$ system driven uniformly (U) and randomly (R) at infinite fields, plotted against T , in units of T_{c0} .

universality class that is entirely different [11] from the Ising case. These results are mainly confirmed in simulation studies [12].

For RDS, the amplitude of the external drive is *uniform* in space but *random* in time. In practice, we simply choose $\pm E$ randomly at each Monte Carlo step (keeping the axis—say, \hat{y} —fixed). Using the same hopping rates as in UDS, we expect, unlike before, *zero current* in the steady state. Nevertheless, the RDS cannot be in an equilibrium state, since energy is constantly fed into the system via jumps along E , and lost to the heat bath via transverse jumps. Since the microscopic dynamics of UDS and RDS are quite distinct, we expect significant differences in the typical thermodynamic quantities other than the particle current. But, much to our surprise, when simulations of the RDS were carried out [13] and compared (Figs. 1–3), there was hardly any difference in the order parameters (as defined in [1,2]), the structure factors (for the lowest transverse and longitudinal momenta), and the internal energies (in terms of the broken

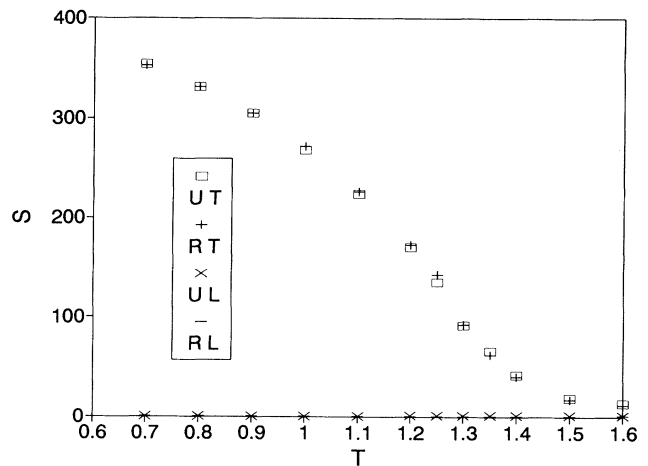


FIG. 2. Transverse (T) and longitudinal (L) structure factors in a $L = 30$ system driven uniformly (U) and randomly (R) at infinite fields.

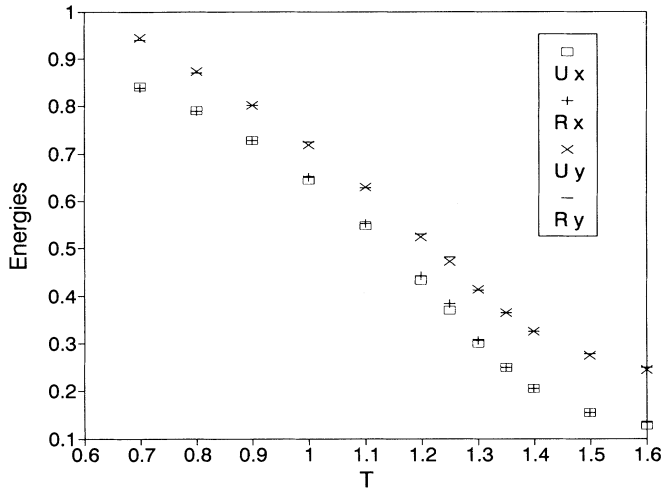


FIG. 3. Internal energies stored in broken x and y bonds, in a $L=30$ system, driven uniformly (U) and randomly (R) with infinite fields.

x and y bonds). Since, for these two systems, we expect quite different universality classes [4], let alone nonuniversal quantities like the critical temperature, we are faced with an intriguing puzzle. Though more refined data do show small differences [13], it would be desirable to measure quantities that provide a higher contrast between these systems. Thus motivated, we study the three-point correlation function, which exploits the symmetry differences to the fullest extent.

III. SYMMETRY DIFFERENCES

Symmetries play an important role in the modeling of physical systems. They are useful for predicting general properties of macroscopic thermodynamic functions, given a particular microscopic dynamics. Beyond that, they form the foundation for determining both an appropriate coarse-grain continuum theory and the universality classes of critical behavior. We devote this brief section to the different symmetries encountered in the two driven systems.

For a UDS in *steady state*, the system is invariant under *any pair* of the following three transformations:

$$s \rightarrow -s, \quad E \rightarrow -E, \quad \text{and} \quad y \rightarrow -y, \quad (3.1)$$

where the first denotes a global change of the spins while y is the coordinate along the drive direction. Thus, the first pair of transformations is equivalent to the statement that E drives particles ($s=+1$) one way and holes ($s=-1$) the opposite way. While the last pair is also obvious, we could combine these into an important, but more subtle, symmetry, i.e., invariance under

$$s \rightarrow -s \quad \text{together with} \quad y \rightarrow -y. \quad (3.2)$$

Since particle-hole interchange is also known as charge conjugation and $y \rightarrow -y$ is a parity transformation, we will refer to this operation as CP .

By contrast, for an RDS in steady state, the randomness of E means that both C and P are separately

preserved. Thus, the symmetry is identical to the Ising symmetry characterized by invariance under $s \rightarrow -s$, in particular. We should remark that, for either system below criticality, the physics is more complex, since the symmetries under both C and *translation* are spontaneously broken, the latter being a result of the particle-conserving dynamics.

Thus, the consequence of this difference between the symmetries of the UDS and the RDS is most transparent for $T > T_c$, where they remain unbroken. Under C , *any* equal-time correlation of an odd number of spins is the negative of itself and, therefore, must vanish. On the other hand, CP requires only that such correlations must be odd under P (in y). Since $\langle s \rangle \equiv 0$ by our dynamics, the simplest correlation function which exploits this distinction is the three-point function. To summarize, we expect, on grounds of symmetry alone,

$$\begin{aligned} \langle s(x_1, y_1) s(x_2, y_2) s(x_3, y_3) \rangle \\ = - \langle s(x_1, -y_1) s(x_2, -y_2) s(x_3, -y_3) \rangle \end{aligned} \quad (3.3)$$

for a UDS, but

$$\langle sss \rangle \equiv 0 \quad (3.4)$$

for an RDS.

IV. THEORY OF THE THREE-POINT FUNCTION

A convenient and powerful medium for discussing theoretical approaches is continuum field theory, which is known to provide a good approximation for describing the long-wavelength properties of thermodynamic systems. Instead of discrete spins on discrete space-time, we now consider a coarse-grained version, the local magnetization $\phi(\mathbf{x}, t)$, in continuous space-time. Instead of the master equation (2.2), we will use an equation of motion for ϕ itself, together with noise terms. Known as a Langevin equation, an appropriate choice requires careful consideration of the essential physics, e.g., conservation laws and symmetries. The spirit behind such an approach is the same as studying a Landau-Ginzburg-Wilson Hamiltonian [14]:

$$\mathcal{H}[\phi] = \int d^d x \left[\frac{\kappa}{2} (\nabla \phi)^2 + \frac{\tau}{2} \phi^2 + \frac{u}{4!} \phi^4 \right], \quad (4.1)$$

instead of the microscopic (2.1). This route proved to be especially successful in the understanding of dynamics in the critical region [15].

Since particle number is conserved in our dynamics, we begin with the continuity equation

$$\frac{\partial}{\partial t} \phi(\mathbf{x}, t) + \nabla \cdot \mathbf{j}(\mathbf{x}, t) = 0, \quad (4.2)$$

where \mathbf{j} is the local particle current. For a system evolving under the influence of \mathcal{H} , a simple choice is

$$\mathbf{j}(\mathbf{x}, t) = -\lambda \nabla \frac{\partial \mathcal{H}}{\partial \phi} + \xi, \quad (4.3)$$

where λ is an Onsager coefficient and ξ is a random noise, representing thermal fluctuations. For most physical sys-

tems, λ would be ϕ dependent. However, focusing mainly on behavior for small ϕ , we will approximate it by a constant. The first term in (4.3) models the systematic evolution of $\phi(\mathbf{x}, t)$ towards configurations with minimal energy. For the noise, we postulate independent Gaussian distributions at each (\mathbf{x}, t) , with zero mean:

$$\begin{aligned} \langle \xi \rangle &= 0, \\ \langle \xi_i(\mathbf{x}, t) \xi_j(\mathbf{x}', t') \rangle &\propto \delta_{ij} \delta(\mathbf{x} - \mathbf{x}') \delta(t - t'). \end{aligned} \quad (4.4)$$

These are the ingredients for model-B critical dynamics [15].

Next, we include the effects of a *uniform* drive by adding a third term,

$$\sigma[\rho(x, t)] \mathcal{E} \hat{y}, \quad (4.5)$$

which represents the current due to E . Generally, the conductivity σ depends on the local particle density $\rho(\mathbf{x}, t)$, which is related to ϕ via $\phi = 2\rho - 1$. Unlike the case for λ , approximating σ by a constant alone is clearly insufficient, since such a term will disappear from (4.2). Now, an essential part of the ρ dependence should take into account the vanishing of j if all sites are fully occupied or vacant, i.e., $\rho = 1$ or 0 . The simplest such dependence is $\sigma \propto \rho(1 - \rho)$, i.e.,

$$\sigma[\phi] \propto (1 - \phi^2). \quad (4.6)$$

Finally, we comment that the \mathcal{E} in (4.5) is not identical, though closely related, to E . For example, \mathcal{E} must be an odd function of E . Also, since the particle density and average velocity remain finite even if $E \rightarrow \infty$, we expect \mathcal{E} to saturate at some finite value in that limit. It is best to regard \mathcal{E} as some function of the microscopic parameters E , J , and β , which arises from the coarse-graining process.

Combining (4.1), (4.2), (4.3), and (4.5), we arrive at an *isotropic* equation of motion:

$$\partial_t \phi = \lambda \nabla^2 \{ (\tau - \kappa \nabla^2) \phi + u \phi^3 / 3! \} - \nabla \cdot \xi + \mathcal{E} \nabla^2 \phi^3.$$

However, a very important effect of the drive is the introduction of *strong anisotropy*. We will use the term ‘‘longitudinal’’ to refer to the direction along E . Denoting transverse gradients by ∇ and longitudinal ones by ∂ , we write the fully anisotropic Langevin equation

$$\begin{aligned} \frac{\partial}{\partial t} \phi(\mathbf{x}, t) &= \lambda \{ \nabla^2 (\tau_\perp - \kappa_\perp \nabla^2) + \partial^2 (\tau_\parallel - \kappa_\parallel \partial^2) - \kappa_\times \partial^2 \nabla^2 \} \phi \\ &+ \mathcal{E} \partial \phi^2 + (u_\perp \nabla^2 + u_\parallel \partial^2) \phi^3 / 3! - (\nabla \cdot \xi + \partial \zeta). \end{aligned} \quad (4.7)$$

Note that the noise term has also been generalized to accommodate anisotropy. Instead of (4.4), we allow different correlations for the transverse components ξ and the longitudinal part ζ . A compact form for these is

$$\begin{aligned} \langle \nabla \cdot \xi(\mathbf{x}, t) \nabla' \cdot \xi(\mathbf{x}', t') \rangle &= -2\eta_\perp \nabla^2 \delta(\mathbf{x} - \mathbf{x}') \delta(t - t'), \\ \langle \partial \zeta(\mathbf{x}, t) \partial' \zeta(\mathbf{x}', t') \rangle &= -2\eta_\parallel \partial^2 \delta(\mathbf{x} - \mathbf{x}') \delta(t - t'). \end{aligned} \quad (4.8)$$

While we argue that (4.7) is an appropriate Langevin equation for UDS, it cannot be the proper choice for RDS. In the latter, the randomness in E will ‘‘wash out’’ a term like $\mathcal{E} \partial \phi^2$. On the other hand, strong anisotropy should still be present, so that there is not reason to expect coefficients like τ_\perp and τ_\parallel to be degenerate. Thus, we propose, for RDS, a Langevin equation which is (4.7) minus the $\mathcal{E} \partial \phi^2$ term. In both cases, we neglected terms with higher powers of ϕ and gradients, since we attempt to describe only the long-wavelength properties of small fluctuations.

Before continuing to compute the three-point correlation function within this theoretical framework, we remark that these equations possess the same CP versus C symmetries discussed above. It is clear that, without the $\mathcal{E} \partial \phi^2$ term, (4.7) is invariant under $\phi \rightarrow -\phi$, since there are only odd powers of ϕ in all terms. On the other hand, the extra $\mathcal{E} \partial \phi^2$ certainly violates this symmetry, while displaying clearly the invariance under CP , or the other pairs of transformations in (3.1). Respecting C symmetry, our theory for RDS will naturally predict a vanishing three-point function. In the remainder of this section, we concentrate on the nontrivial UDS case.

We now consider the correlation of three particles at equal times. Since time-translational invariance holds in the steady state, we may write a function independent of t :

$$G(x_1, x_2, x_3) \equiv \langle \phi(x_1, t) \phi(x_2, t) \phi(x_3, t) \rangle, \quad (4.9)$$

where the average is taken over the Gaussian distribution of the noise. Thus, in principle, we must solve (4.7) for each realization of (ξ, ζ) and then perform the averages. In practice, it is much easier to recast (4.7) in terms of functional integrals, by introducing a Martin-Siggia-Rose [16] response field $\tilde{\phi}$. Specifically, averages are given by

$$\langle \dots \rangle = \int \mathcal{D}\phi \mathcal{D}\tilde{\phi} \dots \exp(-\mathcal{J}[\tilde{\phi}, \phi]), \quad (4.10)$$

where

$$\mathcal{J}[\tilde{\phi}, \phi] = \int d^d x dt \{ \tilde{\phi} [\partial_t \phi - F(\phi)] + \eta_\parallel \tilde{\phi} \partial^2 \tilde{\phi} + \eta_\perp \tilde{\phi} \nabla^2 \tilde{\phi} \}, \quad (4.11)$$

and $F(\phi)$ is just the systematic part of the Langevin equation (4.7). Note that, in this formalism [17], the dynamic functional \mathcal{J} plays the same role as $\beta\mathcal{H}$ in an equilibrium canonical ensemble.

Both the response and the correlation functions of this theory may be summarized in the generating functional

$$Z[\tilde{h}, h] \equiv \int \mathcal{D}\phi \mathcal{D}\tilde{\phi} \exp\{-\mathcal{J}[\tilde{\phi}, \phi] + \int (h \cdot \tilde{\phi} + \tilde{h} \cdot \phi)\}, \quad (4.12)$$

so that *truncated* correlation functions (known as connected Green’s functions in field theory) are simply functional derivatives of

$$W \equiv \ln Z, \quad (4.13)$$

with respect to the ‘‘source’’ $\tilde{h}(\mathbf{x}, t)$. Focusing in particular on the three-point function above T_c , where $\langle \phi \rangle \equiv 0$, we see that it is identical to the truncated correlation.

Thus

$$G(\mathbf{x}_1, \mathbf{x}_2, \mathbf{x}_2) = \frac{\delta}{\delta \tilde{h}(\mathbf{x}_1, t)} \frac{\delta}{\delta \tilde{h}(\mathbf{x}_2, t)} \frac{\delta}{\delta \tilde{h}(\mathbf{x}_2, t)} W[\tilde{h}, h] \Big|_{h=0, \tilde{h}=0}. \quad (4.14)$$

Of course, (4.14) is only a formal expression, while an actual computation would proceed via perturbation theory.

In this approach, the weight in (4.12) is separated into a Gaussian part and a non-Gaussian part, which is treated in a perturbation expansion. Note that this is equivalent to treating the nonlinear terms in (4.7) perturbatively. The generating functional for the Gaussian part is easily found, especially in the space of momenta and frequencies $K \equiv (\mathbf{k}, \omega)$. Begin with the definition

$$Z_0[\tilde{h}, h] \equiv \int \mathcal{D}\phi \mathcal{D}\tilde{\phi} \exp \left\{ \int dK [\frac{1}{2}\Phi^\dagger \mathcal{G}^{-1} \Phi + H^\dagger \Phi] \right\}, \quad (4.15)$$

where $dK \equiv d^d k d\omega$. We have also combined the two fields into vector form:

$$\Phi \equiv \begin{bmatrix} \tilde{\phi}(\mathbf{k}, \omega) \\ \phi(\mathbf{k}, \omega) \end{bmatrix} \quad \text{and} \quad H \equiv \begin{bmatrix} h(\mathbf{k}, \omega) \\ \tilde{h}(\mathbf{k}, \omega) \end{bmatrix}, \quad (4.16)$$

with

$$\mathcal{G}^{-1} = \begin{bmatrix} 2\Sigma(k) & i\omega - \Gamma(k) \\ -i\omega - \Gamma(k) & 0 \end{bmatrix}, \quad (4.17)$$

where

$$\Sigma(k) \equiv \eta_{\parallel} k_{\parallel}^2 + \eta_{\perp} k_{\perp}^2 \quad (4.18a)$$

and

$$\Gamma(k) \equiv \tau_{\parallel} k_{\parallel}^2 + \tau_{\perp} k_{\perp}^2 + \kappa_{\parallel} k_{\parallel}^4 + \kappa_{\times} k_{\parallel}^2 k_{\perp}^2 + \kappa_{\perp} k_{\perp}^4. \quad (4.18b)$$

A Gaussian transformation leads to

$$Z_0[\tilde{h}, h] \propto \exp \left\{ \int dK \frac{1}{2} H^\dagger \mathcal{G} H \right\} \quad (4.19)$$

and

$$W_0[\tilde{h}, h] = \int dK \frac{1}{2} H^\dagger \mathcal{G} H, \quad (4.20)$$

where, by inverting (4.17),

$$\mathcal{G}(K) = \frac{1}{\omega^2 + \Gamma^2} \begin{bmatrix} 0 & i\omega - \Gamma(k) \\ -i\omega - \Gamma(k) & -2\Sigma(k) \end{bmatrix}. \quad (4.21)$$

Of course, the three-point function is identically zero at this level, as W_0 is only quadratic in H .

To go beyond the Gaussian approximation, we first consider the effects of \mathcal{E} . The trilinear term in the exponent, $\int \mathcal{E} \tilde{\phi} \partial \phi^2$, may be written in terms of functional derivatives with respect to h and \tilde{h} . In Fourier space, it is explicitly

$$\int dQ_1 dQ_2 dQ_3 \delta(Q_1 + Q_2 + Q_3) \times \mathcal{E}(-iq_{1\parallel}) \frac{\delta}{\delta h(Q_1)} \frac{\delta}{\delta \tilde{h}(Q_2)} \frac{\delta}{\delta \tilde{h}(Q_3)}. \quad (4.22)$$

In this form, it is independent of Φ and can be taken outside the integrals in (4.12). Expanding the exponential in powers of \mathcal{E} , we have

$$Z = \sum_0^{\infty} \frac{1}{N!} \left\{ \int d^3 Q \delta \left[\sum_i Q_i \right] \mathcal{E}(-q_{1\parallel}) \times \frac{\delta}{\delta h(Q_1)} \frac{\delta}{\delta \tilde{h}(Q_2)} \frac{\delta}{\delta \tilde{h}(Q_3)} \right\}^N Z_0. \quad (4.23)$$

To first order in \mathcal{E} , we have

$$Z_1 \equiv \left\{ \int d^3 Q \delta \left[\sum_i Q_i \right] \mathcal{E}(-iq_{1\parallel}) \times \frac{\delta}{\delta h(Q_1)} \frac{\delta}{\delta \tilde{h}(Q_2)} \frac{\delta}{\delta \tilde{h}(Q_3)} \right\} Z_0, \quad (4.24)$$

and, expanding the logarithm,

$$W_1 = Z_1 / Z_0. \quad (4.25)$$

Since $Z_0 = \exp W_0$, we have $\delta Z_0 / \delta H \propto Z_0$ and $Z_1 \propto Z_0$. The proportionality factor is just W_1 and consists of terms like $(\delta^2 W / \delta H^2)(\delta W / \delta H)$ and $(\delta W / \delta H)^3$. Referring to (4.14), we see that only terms of $O(H^3)$ in W_1 are needed. Thus, we have

$$W_1 = \int d^3 Q \delta \left[\sum_i Q_i \right] \mathcal{E}(-iq_{1\parallel}) \times \frac{\delta W_0}{\delta h(Q_1)} \frac{\delta W_0}{\delta \tilde{h}(Q_2)} \frac{\delta W_0}{\delta \tilde{h}(Q_3)}. \quad (4.26)$$

Returning to (4.14), we now have the first-order (in \mathcal{E}) contribution to the three-point function in K space:

$$G(K_1, K_2, K_3) = \frac{\delta}{\delta \tilde{h}(K_1)} \frac{\delta}{\delta \tilde{h}(K_2)} \frac{\delta}{\delta \tilde{h}(K_3)} W_1. \quad (4.27)$$

Since each factor $\delta W_0 / \delta H$ in (4.26) is linear in H , the functional derivatives in (4.27) lead to various matrix elements of

$$\delta^2 W_0 / \delta H(Q) \delta H(K) = \mathcal{G}(K) \delta(Q - K).$$

Using subscripts to denote these elements, we arrive at

$$G(K_1, K_2, K_3) = -i \mathcal{E} \delta \left[\sum_i K_i \right] \times \{ k_{1\parallel} \mathcal{G}_{\tilde{\phi}\tilde{\phi}}(K_1) \mathcal{G}_{\phi\phi}(K_2) \mathcal{G}_{\phi\phi}(K_3) + (\text{five permutations}) \}, \quad (4.28)$$

Now, we are interested in the *equal-time* correlation, so the Fourier transform of (4.14) is given by

$$G(k_1, k_2, k_3) = (2\pi)^{-3} \int d\omega_1 d\omega_2 d\omega_3 G(K_1, K_2, K_3). \quad (4.29)$$

Carrying out the integrations with the elements in (4.21), we finally obtain the result

$$G(k_1, k_2, k_3) = \frac{-2i \mathcal{E} \delta(k_1 + k_2 + k_3)}{\Gamma(k_1) + \Gamma(k_2) + \Gamma(k_3)} \times \{k_{1\parallel} S(k_2) S(k_3) + (\text{two permutations})\}, \quad (4.30)$$

where

$$S(k) \equiv \Sigma(k) / \Gamma(k) \quad (4.31)$$

is just the two-point correlation at equal times. That $G(\{k_i\})$ is purely imaginary in momentum space is a reflection of $G(\{x_i\})$ having odd parity.

So far, we have discussed the contributions to the three-point function at the lowest order in perturbation theory, starting from (4.7) and (4.8), namely, to first order in \mathcal{E} and zeroth order in the u 's. At this level, notice that no K integrals are involved, a level known as the tree approximation. In principle, higher-order contributions, in which we encounter loop integrals, can be computed. However, since we are only concerned with the properties at long wavelengths (or small K), we argue that there will be no qualitatively new behavior, except near T_c . Unlike quantum field theory, the lattice spacing provides a natural large- K cutoff. At the other limit, keeping T above T_c gives us infrared cutoffs, so that all the integrals are finite. The effect of higher orders appears simply as (finite) renormalizations of various parameters, e.g., τ , \mathcal{E} , etc. Since we did not attempt to relate these parameters to the microscopic model while regarding (4.7) as a phenomenological theory, such renormalizations are "unimportant." In conclusion, we believe that (4.30) provides the correct small-momenta behavior of the three-point correlation in a uniformly driven system. Before proceeding to simulation studies, we investigate this behavior in some detail.

We first note that a formula like (4.30) has been derived previously [18]. However, there is one important difference, hidden in (4.31). Unlike our (4.18), the earlier work studied the effects of the drive only to the *lowest* order, so that isotropic $\Sigma(k)$ and $\Gamma(k)$, characteristic of an equilibrium system, were used. This precludes the possibility of a discontinuity singularity in $S(k)$, which is a consequence of the violation of the fluctuation-dissipation theorem (FDT) in nonequilibrium systems [7]. In particular, FDT guarantees [19] that, for systems near equilibrium, $\eta_{\perp} / \tau_{\perp} = \eta_{\parallel} / \tau_{\parallel}$, i.e., a special relationship between the noise correlations and the diffusive coefficients. Though we are interested in a steady state, we should expect the nonequilibrium character to break the FDT *generically*. That is, we expect

$$R \equiv \frac{\eta_{\perp} \tau_{\parallel}}{\tau_{\perp} \eta_{\parallel}} = \frac{S(\mathbf{k}_{\perp} \rightarrow \mathbf{0}, k_{\parallel} = 0)}{S(\mathbf{k}_{\perp} = \mathbf{0}, k_{\parallel} \rightarrow 0)} \neq 1 \quad (4.32)$$

for all $T > T_c$. Indeed, the data in Fig. 2 illustrate the inequality of these two limits well, where $S(\mathbf{k}_{\perp} \rightarrow \mathbf{0}, k_{\parallel} = 0)$ is labeled as the "transverse structure factor" and $S(\mathbf{k}_{\perp} = \mathbf{0}, k_{\parallel} \rightarrow 0)$, the "longitudinal" one. In other stud-

ies, R is observed to be generally greater than 1, approaching unity as $T \rightarrow \infty$. Note also that, if $R = 1$, the $O(k^2)$ terms in $S(k)$ cancel and the familiar Ornstein-Zernike form $1/[1 + O(k^2)]$ is recovered.

Returning to (4.30), we see that, if isotropic S 's were used, the factor in the $\{ \}$ brackets approaches

$$\{(k_1 + k_2 + k_3)_{\parallel} + O(k^3)\}$$

as $k \rightarrow 0$. Since the δ function forces the first term to be zero and Γ is $O(k^2)$, we conclude that G vanishes as $O(k)$. This is indeed the conclusion of [18]. On the other hand, if $S(k \rightarrow 0)$ is $O(1)$, which depends on the *angle* of \mathbf{k} , then generically the permutations will not produce the simple sum at $O(k)$, leading to G diverging as $O(1/k)$ typically. Of course, for special momenta, e.g., all transverse, G *vanishes identically*. Thus, we are led to conclude that $G(\{k_i\})$ has an infinite discontinuity in the limit of small \mathbf{k} . Of course, for finite systems, k is bounded from below by $2\pi/L$, so that the maximum discontinuity is $O(L)$ in that case.

Since G is a function of two (independent) momenta, to measure it fully by Monte Carlo simulations would require considerable computer time. Instead, we propose to study quantities derived from G , denoted by \mathcal{G} and g , chosen for their simplicity and to accentuate the effects of FDT violation. Maximizing the difference between the three momenta, we choose \mathbf{k}_1 to be purely longitudinal and \mathbf{k}_2 to be purely transverse. From the δ function, we have $k_{3\parallel} = -k_{1\parallel}$ and $\mathbf{k}_{3\perp} = -\mathbf{k}_{2\perp}$. The three permutations in (4.30) reduce to two terms and the result is proportional to $\{S(k_3) - S(k_1)\}$, which would have vanished if S had no discontinuity at $k = 0$. Choosing $k_{1\parallel} = |\mathbf{k}_{2\perp}| \equiv k$ and keeping only the lowest-order term, we find

$$\mathcal{G}(k) = -i \frac{\mathcal{E}}{k} (R - 1) \frac{\eta_{\parallel} \eta_{\perp}}{\tau_{\parallel} (\tau_{\parallel} + \tau_{\perp})^2} + O(k). \quad (4.33)$$

Note that, by setting $\mathbf{k}_2 = -\mathbf{k}_1 - \mathbf{k}_2$, there would be a factor $\delta(0)$ in G . But this is just the spatial volume of the system, coming from a sum over a translationally invariant quantity. Dropping this factor in defining \mathcal{G} , we see that it displays all the essential features of our three-point function, namely, it (i) vanishes with \mathcal{E} ; (ii) diverges as $O(1/k)$ for small generic k ; (iii) is proportional to the FDT violating $R - 1$; (iv) is purely imaginary; and (v) is negative, given that $R > 1$ is generally observed. We will see that even relatively crude simulations confirm these predictions.

Another special quantity is obtained, instead of setting the transverse momentum equal to $k_{1\parallel}$, by integrating over $\mathbf{k}_{2\perp}$. This operation corresponds, in real space, simply to setting a pair of transverse coordinates equal. The result is a function of a single variable:

$$g(p) = -2i \mathcal{E} p \int \frac{d^{d-1} \mathbf{q}}{(2\pi)^{d-1}} \frac{S(\mathbf{q}) \{S(p, \mathbf{q}) - S(p)\}}{\Gamma(p) + \Gamma(\mathbf{q}) + \Gamma(p, \mathbf{q})}, \quad (4.34)$$

where $p \equiv k_{1\parallel}$, $\mathbf{q} \equiv \mathbf{k}_{2\perp}$, and $\delta(0)$ is again dropped. Though it is straightforward to perform the integration, the final form is not very illuminating, even for $d = 2$. Instead, we simply note that the distinguishing features list-

ed above are still present, with the exception of (ii). The integration softens this singularity, so that $g(p)$ approaches a constant (in $d=2$).

Finally, we remark that the analysis for T below T_c has yet to be carried out. There are several complications: the first is the spontaneous breakdown of both Ising and Euclidean symmetry: $\langle \phi(\mathbf{x}) \rangle \neq 0$. Perturbation theory must now be set up around an inhomogeneous steady state which characterizes a phase-separated state. Of course, we can remark on the simple case of $T=0$, where no fluctuations exist and the three-point correlation vanishes.

V. SIMULATION RESULTS

Our simulations are performed on two-dimensional square lattices of linear dimensions $L=10, 30$, and 60 . All initial configurations are half-filled and random, corresponding to $T=\infty$. At lower temperatures, we update in the following manner: First, a site is chosen randomly, followed by a random choice of one of its four nearest neighbors. If the spins of this pair of sites are different, then we evaluate the difference in energy between the original configuration and the configuration after spin exchange. Finally, the two spins will be exchanged or not, according to the Metropolis rate

$$\min\{1, \exp[-\beta(\Delta\mathcal{H} + \epsilon E)]\}.$$

A Monte Carlo Step (MCS) denotes L^2 such attempts, so that, in a MCS, each site will be visited once on average. For UDS, E is fixed for the entire run, while for RDS, the *sign* of E is randomly chosen after each MCS. Since larger fields produce larger effects of FDT violation, we used mostly infinite fields, which simply means that jumps against (along) the drive are always forbidden (allowed). Though we have simulated with low fields ($E=4J$), we will not present these data, as they are qualitatively similar to the large-field results. Typically, we discard the initial 10^4 MCS to avoid transients. Then, the physical quantities are measured using configurations separated by 10^3 MCS. The length of the runs range from 2×10^5 to 2×10^6 MCS. We next discuss the results, shown in Figs. 4–10. All temperatures shown are expressed in units of the Onsager T_{c0} .

On a square lattice, the coordinates $\mathbf{x}=(x,y)$ take integer values. We choose to have E point in the positive y direction. For a finite system, k takes the values $2m\pi/L$. Thus, we measure, for the three-point function \mathfrak{G} ,

$$\mathfrak{G}(m) \equiv L^{-2} \sum e^{i(y_1+x_2-y_3-x_3)(2m\pi/L)} \times \langle s(\mathbf{x}_1)s(\mathbf{x}_2)s(\mathbf{x}_3) \rangle, \quad (5.1)$$

where the sum is over all $\{\mathbf{x}_i\}$. Similarly, for g , we use

$$g(m) \equiv L^{-2} \sum e^{i(y_1-y_3)(2m\pi/L)} \delta(x_2, x_3) \times \langle s(\mathbf{x}_1)s(\mathbf{x}_2)s(\mathbf{x}_3) \rangle, \quad (5.2)$$

where δ is the Kronecker delta. Note that both are complex, in principle.

The simulation results of the latter, with $E=\infty$, are shown in Figs. 4–6. In the first, we plot $g(1)$, for both

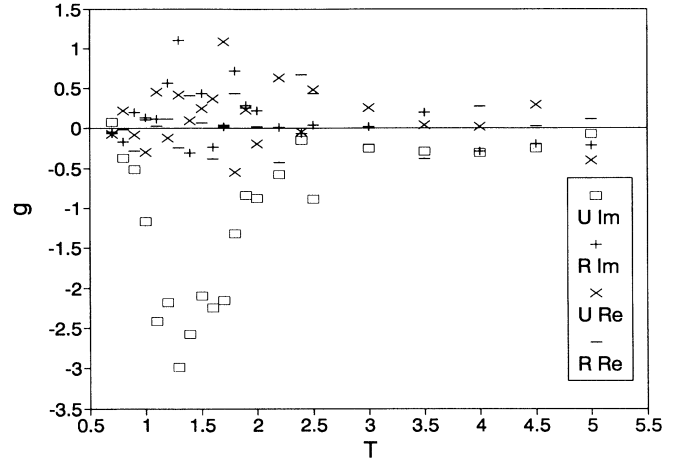


FIG. 4. Imaginary and real parts of the three-point function g , in a $L=30$ system, driven uniformly (U) and randomly (R) with infinite fields.

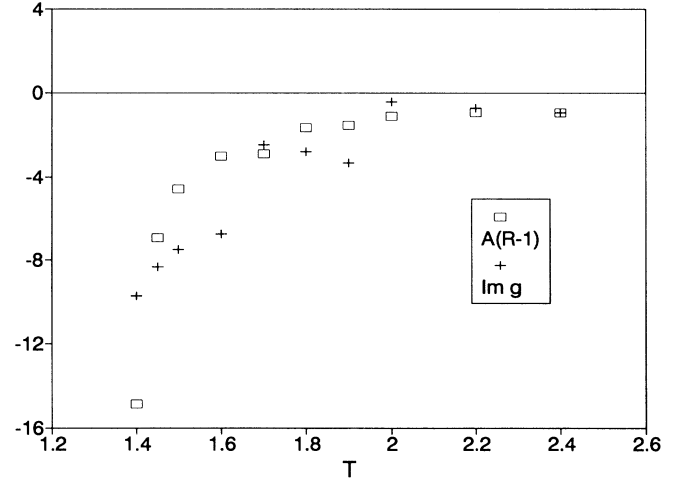


FIG. 5. A comparison between the measured $\text{Im}(g)$ in Fig. 4 and the FDT violating parameter $(R-1)$, taken from the data in Fig. 2.

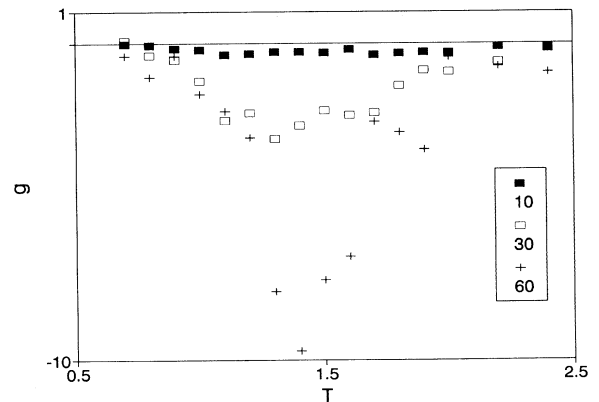


FIG. 6. $\text{Im}(g)$ as a function of T in $L=10, 30$, and 60 systems driven uniformly with infinite fields.

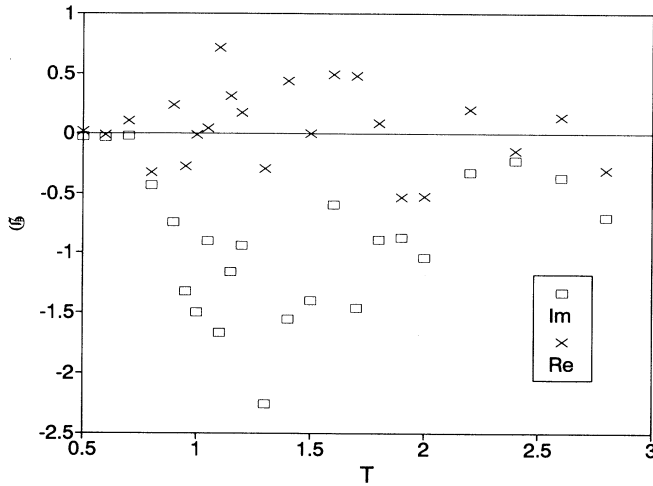


FIG. 7. Imaginary and real parts of \mathcal{G} in a $L=10$ system driven uniformly with infinite fields.

UDS and RDS on a 30×30 lattice against T . Of the four curves, only the imaginary part of g in the UDS is statistically nonzero. Note that it is negative, as predicted. Focusing on the part above T_c , i.e., $T \gtrsim 1.41$, we see that its magnitude decreases with T . To understand, at least roughly, this behavior, we recall that $g \propto (R-1)$, which displays a similarly strong variation with T . In Fig. 5, we compare the data with $A(R-1)$, where A is a fitted parameter and R comes from the structure-factor data. Though better statistics is obviously needed for making quantitative conclusions, these curves provide good evidence for the properties (iii)–(v) listed above. In Fig. 6, we show only $\text{Im}[g(1)]$ in UDS of three different sizes: $L=10, 30$, and 60 . Again, we can understand, qualitatively, this L dependence. Since $m=1$ corresponds to $k=2\pi/L$, these three curves reflect probing g at different k 's. Recalling property (ii) above, we see that the increasing magnitude with L is consistent with the diverging $1/k$ dependence.

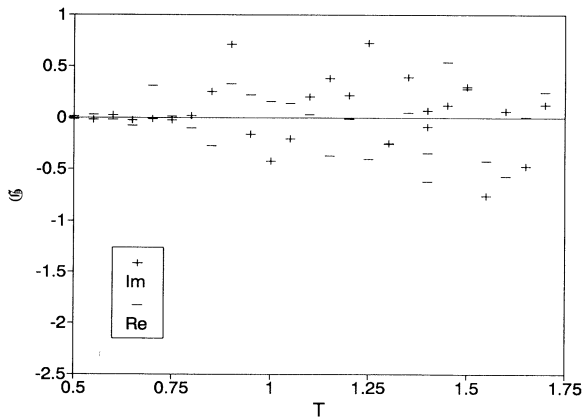


FIG. 8. Imaginary and real parts of \mathcal{G} in a $L=10$ system driven randomly with infinite fields.

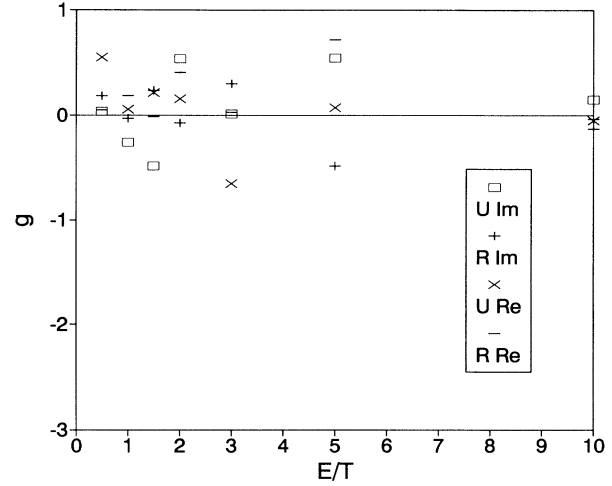


FIG. 9. Three-point function in a $L=30$ system of noninteracting particles, driven with various fields.

In Figs. 7 and 8, we show $\mathcal{G}(1)$ versus T , for UDS and RDS, respectively. In the latter, we concentrated on a temperature range near T_c where the effects might be largest. Due to the extra Fourier transform, we are limited by time to study only a $L=10$ system. As a result, the magnitude of the three-point function is rather small. Nevertheless, we believe the data confirm that all are consistent with zero, *except* for $\text{Im}(\mathcal{G})$ in a UDS, which displays most of the characteristics predicted.

The next two figures show the effects on $g(1)$ due to turning off either the interparticle interaction ($J=0$) or the drive ($E=0$). In both cases, the three-point function vanishes. While the latter (Fig. 10) is a check on the expected behavior of an equilibrium Ising model, the former result (Fig. 9) is less obvious. To see this result, it is necessary to check that the steady-state distribution for a $J=0$ system is uniform, i.e., $P(C)=1$ solves (2.2) with zero on the left.

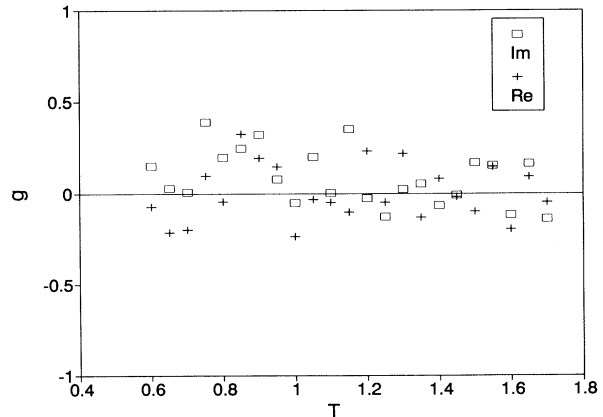


FIG. 10. Three-point function in a $L=30$ system of interacting particles, with zero drive.

VI. SUMMARY AND OUTLOOK

In simulation studies of Ising lattice-gas models driven by external fields, it seems that the routinely measured quantities, such as structure factors, order parameters, and internal energies, cannot distinguish an important aspect of the drive, i.e., whether it is uniform or random (with zero mean). Yet, it is clear that there are major differences between the symmetries underlying these two systems. In particular, the up-down symmetry of the equilibrium Ising model is absent in the former and preserved in the latter. For the uniformly driven case, this symmetry is replaced by *CP*. Exploiting this difference, we study the three-point correlation function, which would be identically zero if the Ising symmetry is obeyed and nontrivial if only *CP* is unbroken.

Being interested only in the long-wavelength limit, where the details of the microscopies are supposedly unimportant, we turn to the framework of continuum field theory of statistical mechanics. However, Hamiltonians and Boltzmann distributions are inadequate for dealing with steady states far from equilibrium. Instead, following the Langevin approach, we propose two diffusive equations of motion for these models. Since the drive is uniaxial, we introduce anisotropic parameters for diffusion coefficients and noise correlations. Further, recognizing that, in general, the fluctuation-dissipation theorem does not apply in nonequilibrium systems, we lift the constraint on these parameters. One of the dramatic consequences, observed in simulation studies, is the existence of a finite discontinuity singularity at the origin of the structure factor, for all temperatures above T_c .

Within this context, we study the three-point correlation function in the uniformly driven case in some detail. We find an *infinite* discontinuity, for all T above T_c , at the origin of the two independent momenta. Of course, for finite systems, no infinities can be present. Instead, the discontinuity is predicted to diverge with L , the linear size of the system. The data from simulation studies mostly confirm our predictions, although better statistics from longer runs in larger systems are needed before quantitative conclusions can be drawn.

We end with an outlook for the future. On the simulations front, there is the obvious need of more refined and more complete data on $G(\{k_i\})$. Beyond, we should measure correlations at unequal times, to map the entire $G(\{K_i\})$. From that and the data on two-point functions, it is possible to extract all the three-point *vertex*

functions, of which there are several. We present above only the one associated with a term like $\mathcal{E}\bar{\phi}\partial\phi^2$, while others remain to be measured.

On the theory front, there are also many unanswered questions. Already mentioned is the problem of analyzing the three-point function below criticality. From simulations, we see that there are dramatic “dips” associated with T_c . However, we believe that they reflect more the singularities of the two-point functions, e.g., $R \rightarrow \infty$, than those in the three-point *vertices*. It is straightforward to use renormalization-group techniques, which proved so successful in finding critical singularities [11], to compute the singularities in these vertices. Clearly, it would be extremely interesting to see if the good agreement between field-theoretic predictions of critical exponents [11] and simulation data [10] continues to hold for the universal singular behavior in three-point functions.

Finally, a most important question is, how can a three-point correlation be observed in physically realizable driven systems? Measuring the two-point correlation function or the structure factor is routine in scattering experiments. In contrast, very little in the literature [20] is devoted to the measurements of higher correlations. One source of the difficulty is that a complete measurement of an N -point correlation requires monitoring $N-1$ momenta, whereas, in a simple scattering experiment, there is only one momentum (transfer) variable. Thus, though the higher terms in, e.g., the Born series can lead to higher correlations, analyzing depolarized light could provide only limited information. It would be most desirable to develop techniques to explore three-point correlations in a wider context, apart from the spectacular features they display in driven diffusive systems.

ACKNOWLEDGMENTS

We thank S. Dietrich, P. A. Egelstaff, H. L. Frisch, J. R. Heflin, G. Indebetouw, J. L. Lebowitz, K.-t. Leung, R. D. Mountain, O. G. Mouritsen, H. Wagner, and D. A. de Wolf for illuminating discussions on measuring three-point functions, and especially K.-t. Leung for his help with simulations. This research is supported in part by grants from the Jeffress Memorial Trust and the National Science Foundation through the Division of Materials Research.

-
- [1] S. Katz, J. L. Lebowitz, and H. Spohn, *Phys. Rev. B* **28**, 1655 (1983).
 - [2] S. Katz, J. L. Lebowitz, and H. Spohn, *J. Stat. Phys.* **34**, 497 (1984).
 - [3] *Solid Electrolytes*, edited by S. Geller, Topics in Applied Physics Vol. 21 (Springer, Heidelberg, 1979); *Fast Ionic Transport in Solids*, edited by J. B. Bates and G. C. Farrington (North-Holland, New York, 1981); *The Physics of Superionic Conductors and Electrode Materials*, edited by J. W. Perram (Plenum, New York, 1983).
 - [4] B. Schmittmann and R. K. P. Zia, *Phys. Rev. Lett.* **66**, 357

- (1991).
- [5] H. Larsen, E. Praestgaard, B. Schmittmann, and R. K. P. Zia (unpublished).
- [6] K. Hwang, B. Schmittmann, and R. K. P. Zia, *Phys. Rev. Lett.* **67**, 326 (1991).
- [7] R. K. P. Zia, K. Hwang, K.-t. Leung, and B. Schmittmann, in *Computer Simulation Studies in Condensed Matter Physics*, edited by D. P. Landau, K. K. Mon, and H.-B. Schüttler (Springer-Verlag, Berlin, 1993), Vol. V.
- [8] E. Ising, *Z. Phys.* **31**, 253 (1925); C. N. Yang and T. D.

- Lee, *Phys. Rev.* **87**, 404 (1952); T. D. Lee and C. N. Yang, *Phys. Rev.* **87**, 410 (1952).
- [9] N. Metropolis, A. W. Rosenbluth, M. M. Rosenbluth, A. H. Teller, and E. Teller, *J. Chem. Phys.* **21**, 1087 (1953).
- [10] K.-t. Leung, *Phys. Rev. Lett.* **66**, 453 (1991).
- [11] H. K. Janssen and B. Schmittmann, *Z. Phys. B* **63**, 517 (1986); K.-t. Leung and J. L. Cardy, *J. Stat. Phys.* **44**, 567 (1986); K. Gawedzki and A. Kupiainen, *Nucl. Phys. B* **269**, 45 (1986). For a review, see B. Schmittmann, *Int. J. Mod. Phys. B* **4**, 2269 (1990).
- [12] See, e.g., B. Schmittmann and R. K. P. Zia, in *Phase Transitions and Critical Phenomena*, edited by C. Domb and J. L. Lebowitz (Academic, New York, in press).
- [13] K. Hwang, Ph.D. thesis, Virginia Polytechnic Institute and State University, 1993.
- [14] D. J. Amit, *Field Theory, the Renormalization Group, and Critical Phenomena*, 2nd ed. (World Scientific, Singapore, 1984).
- [15] B. I. Halperin, P. C. Hohenberg, and S.-K. Ma, *Phys. Rev. B* **10**, 139 (1974). For a review, see P. C. Hohenberg and B. I. Halperin, *Rev. Mod. Phys.* **49**, 435 (1977).
- [16] P. C. Martin, E. D. Siggia, and H. H. Rose, *Phys. Rev. A* **8**, 423 (1973).
- [17] H. K. Janssen, *Z. Phys. B* **23**, 377 (1976); C. de Dominicis, *J. Phys. (Paris) Colloq.* **37**, C247 (1976).
- [18] P. L. Garrido, J. L. Lebowitz, C. Maes, and H. Spohn, *Phys. Rev. A* **42**, 1954 (1990).
- [19] R. Kubo, *Rep. Prog. Phys.* **29**, 255 (1966).
- [20] H. L. Frisch and J. McKenna, *Phys. Rev.* **139**, A68 (1965); R. S. Ruffine and D. A. de Wolf, *J. Geophys. Res.* **70**, 4313 (1965); H. J. Raveché and R. D. Mountain, *J. Chem. Phys.* **57**, 3987 (1972); P. A. Egelstaff, in *Advances in Chemical Physics*, edited by I. Prigogine and S. A. Rice (Interscience, New York, 1983), Vol. 53, p. 1; P. Jacobaeus, J. U. Madsen, F. Kragh, and R. M. J. Cotterill, *Philos. Mag.* **41**, 11 (1980); C. Itzykson and J.-M. Drouffe, *Statistical Field Theory* (Cambridge University, Cambridge, England, 1989); S. Dietrich and W. Fenzl, *Phys. Rev. B* **39**, 8873 (1989).